Dyes and Pigments 108 (2014) 50–56

Contents lists available at ScienceDirect

Dyes and Pigments

journal homepage: www.elsevier.com/locate/dyepig

N,*N*-dimethylamino-phenylene–acetylene scaffolding: Structure–property relationships

Numan Almonasy [a,*], Filip Bureš [a], Miloš Nepraš [a], Hana Přichystalová [a], Günter Grampp [b]

[a] *Institute of Organic Chemistry and Technology, Faculty of Chemical Technology, University of Pardubice, Studentská 573, Pardubice CZ-532 10, Czech Republic*

[b] *Institute of Physical and Theoretical Chemistry, TU Graz, Stremayergasse 9/I, Graz A-8010, Austria*

A R T I C L E I N F O

Article history:
Received 8 March 2014
Received in revised form
3 April 2014
Accepted 14 April 2014
Available online 24 April 2014

Keywords:
Acetylene
Phenylene
π-System
Absorption
Emission
Donor

A B S T R A C T

Seven model donor-substituted phenyleneethynylene molecules with up to three 1,4-phenylene and two acetylenic units were synthesized by Suzuki–Miyaura and Sonogashira cross-coupling reactions and further studied by absorption and emission spectra and theoretical calculations. The π-system between the *N*,*N*-dimethylamino group and terminal acetylene was systematically elongated which allowed elucidation of the fundamental structure–property relationships. Structural factors such as molecular length and chromophore planarity proved to be crucial for the observed spectroscopic behavior.

1. Introduction

Extended and functionalized organic π-conjugated systems are currently attracting great interest by materials scientists [1–3]. Among others, cyclic and linear hydrocarbons, benzene and acetylene represent probably the most essential building blocks for the construction of large scaffolds, systems and poly(*p*-phenyleneethynylene) derivatives (PPE) [4–7]. These two units were widely employed as a part of the π-conjugated systems of various materials for organic photovoltaics (OPVCs) [8,9], organic light emitting diodes (OLEDs) [10,11], dye sensitizing solar cells (DSSCs) [12], sensors and chelating ligands [13,14], acceptor units [15], and active biomolecules [16,17]. The main reason of their popularity in material science can be attributed to direct availability, well-known chemistry and reactivity, and relative stability. Electron donor/acceptor (D/A) substituted π-systems based on (hetero)aromates in combination with multiple bonds known as push–pull chromophores are presently one of the most widely designed, prepared and investigated class of organic π-conjugated materials [15,18,19]. These molecules often contain 1,4-phenylene and acetylenic units connecting donor and acceptor parts and allow direct D–A interaction and intramolecular charge transfer (ICT) [15,20]. Such arrangement assures molecule polarization and accounts for their unique properties. We have recently synthesized donor 4,5-disubstituted pyrazine-2,3-dicarbonitrile push–pull chromophores with systematically extended π-system which comprised of 1,4-phenylene and acetylenic subunits [21]. In these D–π–A molecules, the ICT has been investigated and its impact on the molecular properties has been evaluated. Although several structure–property relationships studies on D–π–A system exist to date [20–24], less attention has been paid to the influence of the donor-substituted part of the molecule (D–π) [25–28]. Hence, in this work we will focus on *N*,*N*-dimethylamino-substituted molecules comprising 1,4-phenylene and acetylenic units with systematically extended π-system length.

2. Experimental

2.1. Materials and methods

The absorption spectra were measured on an UV/Vis Perkin–Elmer Lambda 35 spectrophotometer at room temperature. The steady-state fluorescence spectra were measured on a Perkin–Elmer LS 55 spectrophotometer. The instrument provides corrected excitation spectra directly; the fluorescence spectra were corrected for the characteristics of the emission monochromator and for the

---

* Corresponding author.
E-mail address: numan.almonasy@upce.cz (N. Almonasy).

http://dx.doi.org/10.1016/j.dyepig.2014.04.018
0143-7208/

photomultiplier response. For fluorescence measurements, very weakly absorbing solutions (optical density ~ 0.05 at the exciting wavelength in 1-cm cell) were used. Following spectral-grade solvents were used for the measurements: dibutylether (DBE), ethylacetate (EtAc), acetonitrile (MeCN), and 1,4-dioxane (DO).

The relative fluorescence quantum yields were calculated according to the relations $q_F = n^2 \cdot P \cdot K/A$, where $K = q_{Fs} \cdot A_s/n_s^2 \cdot P_s$; n denotes the reflective index of a solvent, P denotes the fluorescence area, A denotes the absorbance at excitation wavelength, subscript s denotes the values for the used fluorescence standard.

The fluorescence quantum yields of the studied compounds were measured using quinine sulfate ($q_F = 0.54$ in 0.5 mol/L H_2SO_4) [29] as the standard. Deaeration of the samples by bubbling with N_2 did not affect the spectra and q_F; therefore, the data presented here correspond to aerated solutions. By using anthracene as standard for some of the studied compounds we obtained practically identical q_F as for the quinine sulfate standard.

Filtrations through a plug were carried out with silica gel 60 (particle size 0.040–0.063 mm, 230–400 mesh; Merck) and commercially available solvents. Thin-layer chromatography (TLC) was conducted on aluminum sheets coated with silica gel 60 F254, obtained from Merck, with visualization by a UV lamp (254 or 360 nm). Melting points (m.p.) were measured with a Bűchi B-540 melting-point apparatus in open capillaries and were uncorrected. ^1H and ^{13}C NMR spectra were recorded at 400 and 100 MHz, respectively, with a Bruker AVANCE 400 instrument at 25 °C. Chemical shifts are reported in ppm relative to the signal of Me_4Si. The residual solvent signal in the ^1H and ^{13}C NMR spectra was used as an internal reference ($CDCl_3$ 7.25 and 77.23 ppm). IR spectra were recorded with a Perkin–Elmer FTIR Spectrum BX spectrometer. Mass spectra were measured with an LC–MS Micromass Quattro Micro API (Waters) instrument with a direct input (ESI, CH_3OH, mass range 200–1000 Da). Elemental analyses were performed with an EA 1108 Fisons instrument.

Compounds **1**–**3** were synthesized earlier [30], the synthesis of compounds **4**–**7** is shown in Scheme 1 [21], less-substituted complementary analogs **1a**, **2a**–**b**, **3a**–**b**, **4a**–**b** and **7a**–**b** are known compounds.

2.2. General method for Suzuki–Miyaura cross-coupling (compounds 4 and 6)

Compound **9** or **10** (1.0 mmol) and 4-iodophenylethynyltrimethylsilane **8** (300 mg; 1.0 mmol) were dissolved in THF (75 mL) and water (15 mL). Argon was bubbled through the solution for 10 min, whereupon $[PdCl_2(PPh_3)_2]$ (35 mg; 0.05 mmol) and Na_2CO_3 (116 mg; 1.1 mmol) were added, and the reaction mixture was stirred under argon at 65 °C for 5 h. The reaction was diluted with water and extracted with CH_2Cl_2 (3 × 100 mL). The combined organic extracts were dried (Na_2SO_4) and the solvents were evaporated in vacuo. The crude product was purified by filtration through a plug (SiO_2; CH_2Cl_2/hexane 1:1).

2.3. General method for Sonogashira cross-coupling (compounds 5 and 7)

Terminal acetylenes **2** or **3** (1.0 mmol) and 4-iodophenylethynyltrimethylsilane **8** (300 mg; 1.0 mmol) were dissolved in triethylamine (15 mL) and dry THF (100 mL). Argon was bubbled through the solution for 10 min, whereupon $[PdCl_2(PPh_3)_2]$ (35 mg; 0.05 mmol) and CuI (19 mg; 0.1 mmol) were added, and the reaction mixture was stirred under argon at 50 °C for 5 h. The solvents were evaporated in vacuo and the crude product was purified by filtration through a plug (SiO_2; CH_2Cl_2/hexane 1:1).

2.4. General method for TMS-deprotection

TMS-protected acetylene **4**–**7** (0.5 mmol) was dissolved in THF (50 mL), cooled to 0 °C and tetrabutylammonium fluoride trihydrate TBAF (50–100 mg) was added and the reaction mixture was followed by TLC (SiO_2; CH_2Cl_2/hexane 1:1) and stirred for 2–3 h. The reaction was diluted with water (50 mL), extracted with CH_2Cl_2 (3 × 100 mL), the combined organic extracts were dried (Na_2SO_4) and the solvents were evaporated in vacuo. The crude product was purified by filtration through a plug (SiO_2; CH_2Cl_2/hexane 1:1).

2.5. Compound 4

Yellowish solid, overall yield over two steps 81%, $R_f = 0.28$ (SiO_2; CH_2Cl_2/hexane 1:1), m.p. 242 °C (dec.). ^1H NMR (400 MHz, $CDCl_3$, 25 °C): $\delta = 7.65$–7.53 (m, 10H; Ar), 6.81 (d, $^3J(H,H) = 8.8$ Hz, 2H; Ar), 3.12 (s, 1H; CH), 3.00 ppm (s, 6H; $N(CH_3)_2$). ^{13}C NMR (100 MHz, $CDCl_3$, 25 °C): $\delta = 150.3$, 141.5, 140.9, 137.9, 132.8, 128.5, 127.8, 127.5, 126.9, 126.8, 120.9, 83.9, 77.9, 40.8 ppm. IR (neat): $\nu = 1665$, 1595, 1488, 1353, 1198, 945, 809 cm^{-1}. MS (ESI): m/z (%): 298 $[M + 1]^+$. Elemental analysis: calcd (%) for $C_{22}H_{19}N$ (297.39): C 88.85, H 6.44, N 4.71; found C 88.55, H 6.37, N 4.68.

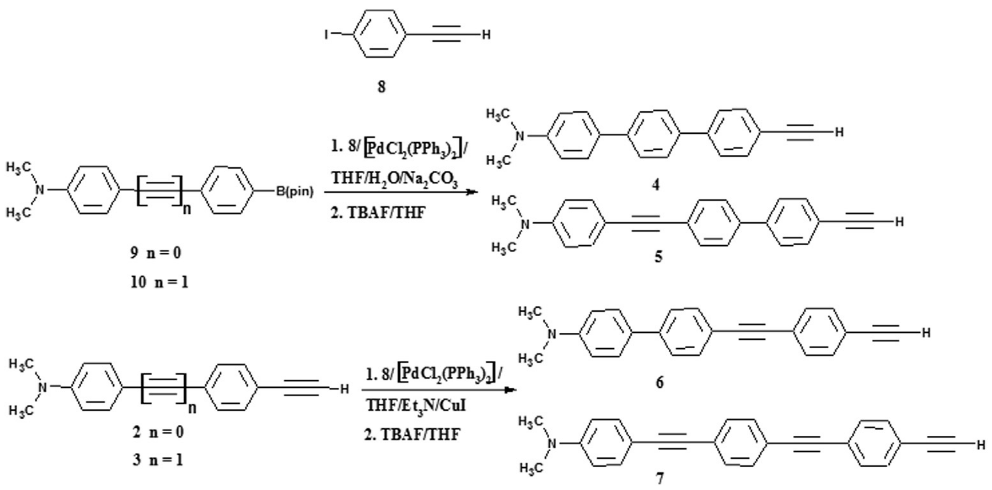

Scheme 1. Synthetic approach to NMe_2-substituted extended p-phenyleneethynylenes **4**–**7**.

2.6. Compound **5**

Yellowish solid, overall yield over two steps 86%, $R_f = 0.32$ (SiO_2; CH_2Cl_2/hexane 1:1), m.p. 216–218 °C. ^1H NMR (400 MHz, $CDCl_3$, 25 °C): $\delta = 7.55–7.45$ (m, 10H; Ar), 6.79 (d, ^3J(H,H) = 8.8 Hz, 2H; Ar), 3.17 (s, 1H; CH), 3.00 ppm (s, 6H; $N(CH_3)_2$). ^{13}C NMR (100 MHz, $CDCl_3$, 25 °C): $\delta = 150.4$, 141.5, 132.3, 132.2, 131.6, 128.1, 127.8, 126.2, 124.2, 121.8, 120.4, 112.9, 92.0, 89.2, 83.6, 79.0, 40.7 ppm. IR (neat): $\nu = 1670$, 1594, 1507, 1346, 1217, 948, 813 cm^{-1}. MS (ESI): m/z (%): 322 $[M + 1]^+$. Elemental analysis: calcd (%) for $C_{24}H_{19}N$ (321.41): C 89.68, H 5.96, N 4.36; found C 89.19, H 5.88, N 4.29.

2.7. Compound **6**

Yellowish solid, overall yield over two steps 82%, $R_f = 0.30$ (SiO_2; CH_2Cl_2/hexane 1:1), m.p. 189–190 °C. ^1H NMR (400 MHz, $CDCl_3$, 25 °C): $\delta = 7.60–7.53$ (m, 8H; Ar), 7.42 (d, ^3J(H,H) = 8.8 Hz, 2H; Ar), 6.66 (d, ^3J(H,H) = 8.8 Hz, 2H; Ar), 3.14 (s, 1H; CH), 2.99 ppm (s, 6H; $N(CH_3)_2$). ^{13}C NMR (100 MHz, $CDCl_3$, 25 °C): $\delta = 150.3$, 141.0, 139.2, 133.0, 132.8, 131.9, 127.0, 127.0, 123.9, 121.3, 112.0, 110.1, 92.0, 87.4, 83.7, 78.1, 40.4 ppm.; IR (neat): $\nu = 1668$, 1595, 1515, 1353, 1136, 944, 818, 776 cm^{-1}. MS (ESI): m/z (%): 322 $[M + 1]^+$. Elemental analysis: calcd (%) for $C_{24}H_{19}N$ (321.41): C 89.68, H 5.96, N 4.36; found C 89.85, H 5.98, N 4.39.

2.8. Compound **7**

Yellowish solid, overall yield over two steps 83%, $R_f = 0.50$ (SiO_2; CH_2Cl_2/hexane 1:1), m.p. 238–239 °C. ^1H NMR (400 MHz, $CDCl_3$, 25 °C): $\delta = 7.46$ (br s, 8H; Ar), 7.40 (d, ^3J(H,H) = 8.8 Hz, 2H; Ar), 6.65 (d, ^3J(H,H) = 8.8 Hz, 2H; Ar), 3.17 (s, 1H; CH), 2.99 ppm (s, 6H; $N(CH_3)_2$). ^{13}C NMR (100 MHz, $CDCl_3$, 25 °C): $\delta = 150.5$, 133.0, 132.3, 131.7, 131.7, 131.4, 124.6, 123.9, 122.1, 121.9, 112.0, 109.8, 93.2, 91.6, 90.5, 87.5, 83.5, 79.2, 40.4 ppm. IR (neat): $\nu = 1606$, 1590, 1520, 1347, 1120, 939, 836, 819 cm^{-1}. MS (ESI): m/z (%): 346 $[M + 1]^+$. Elemental analysis: calcd (%) for $C_{26}H_{19}N$ (345.44): C 90.40, H 5.54, N 4.05; found C 90.77, H 5.60, N 4.09.

Table 1
Molecular structures of the investigated compounds **1**–**7**.

Comp.	Substituents		Central π-linker
	X	Y	
1	NMe_2	C≡CH	
1a	H	C≡CH	
2	NMe_2	C≡CH	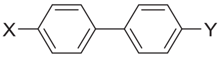
2a	H	C≡CH	
2b	H	H	
3	NMe_2	C≡CH	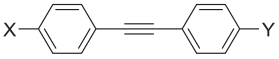
3a	H	C≡CH	
3b	H	H	
4	NMe_2	C≡CH	
4a	H	C≡CH	
4b	H	H	
5	NMe_2	C≡CH	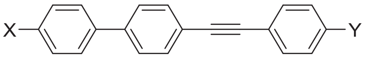
6	C≡CH	NMe_2	
7	NMe_2	C≡CH	
7a	H	C≡CH	
7b	H	H	

3. Results and discussion

3.1. Synthesis

Molecular structure of the studied molecules **1**–**7** is shown in Table 1. Compounds **1**–**3** were synthesized by the methods described in our earlier Ref. [30], the synthesis of extended molecules **4**–**7** is outlined in Scheme 1 and follows protocols shown in Ref. [21] and the experimental part. Two step synthesis involves Suzuki–Miyaura and Sonogashira cross-coupling reactions of boronic acid pinacol esters **9**–**10** [30] and terminal acetylenes **2**–**3** with 4-iodophenylethynyltrimethylsilane **8** [21]. Subsequent trimethylsilyl group removal with tetrabutylammonium fluoride (TBAF) provided desired compounds **4**–**7** in the overall yields of 81–86%. In this way, *N*,*N*-dimethylamino- and ethynyl-terminated molecules with terphenyl (**4**), biphenylethynylphenyl (**5**), phenylethynylbiphenyl (**6**), and phenylethynylphenylethynylphenyl (**7**) systematically evaluated central π-linker were synthesized.

3.2. Absorption spectra

The absorption spectra of the studied compounds are formed by the non-structural broad bands appearing within the range 280–400 nm (Fig. 1, Table 2). Although the changes of the absorption spectra are relatively small, some relationships with the molecular characteristics of studied compounds may be drawn. Despite the molecular length (the distance between the amino nitrogen and the terminal acetylene carbon of the optimized molecule geometry) seems to be the principal structural factor affecting the position of the absorption maxima, the following observations and comparisons must also be taken into account:

- λ_{max} values of compounds **2** and **4** are practically the same even though **4** is longer by one benzene ring; the same relation was found for the compounds **3** and **7**;
- λ_{max} values of **5** and **6** are situated at shorter wavelengths than for **3** even though **5** and **6** are larger;
- by going from **3** to **4**, a strong hypsochromic shift was found whereas compound **4** is longer.

Hence, the observed spectral behavior of **1**–**7** must be elucidated in a more complex manner. As can be seen from Fig. 2 (left), the measured λ_{max} values split into two series (**1**, **2**, and **3**) and (**1**, **4**, **5**, **6**, and **7**) as a dependence on the molecular length. However, structural genesis of these series is not clear especially by going from compound **2** to **3** and from **4** to **7**. The only feature of these series is the molecular length and the number of phenyl rings (two rings for **2** and **3**; three rings for **4, 5**, **6**, and **7**). On the contrary, when considering the structural arrangement of **1**–**7**, they can be divided into two series A and B (Fig. 2). Whereas non-planar chromophores **2** (biphenyl) and **4** (terphenyl) generate series A (practically identical λ_{max} values), planar compounds **1** (phenyl), **3** (phenylethynylphenyl), and **7** (phenylethynylphenylethynylphenyl) belong to series B (strong bathochromic shift of the absorption

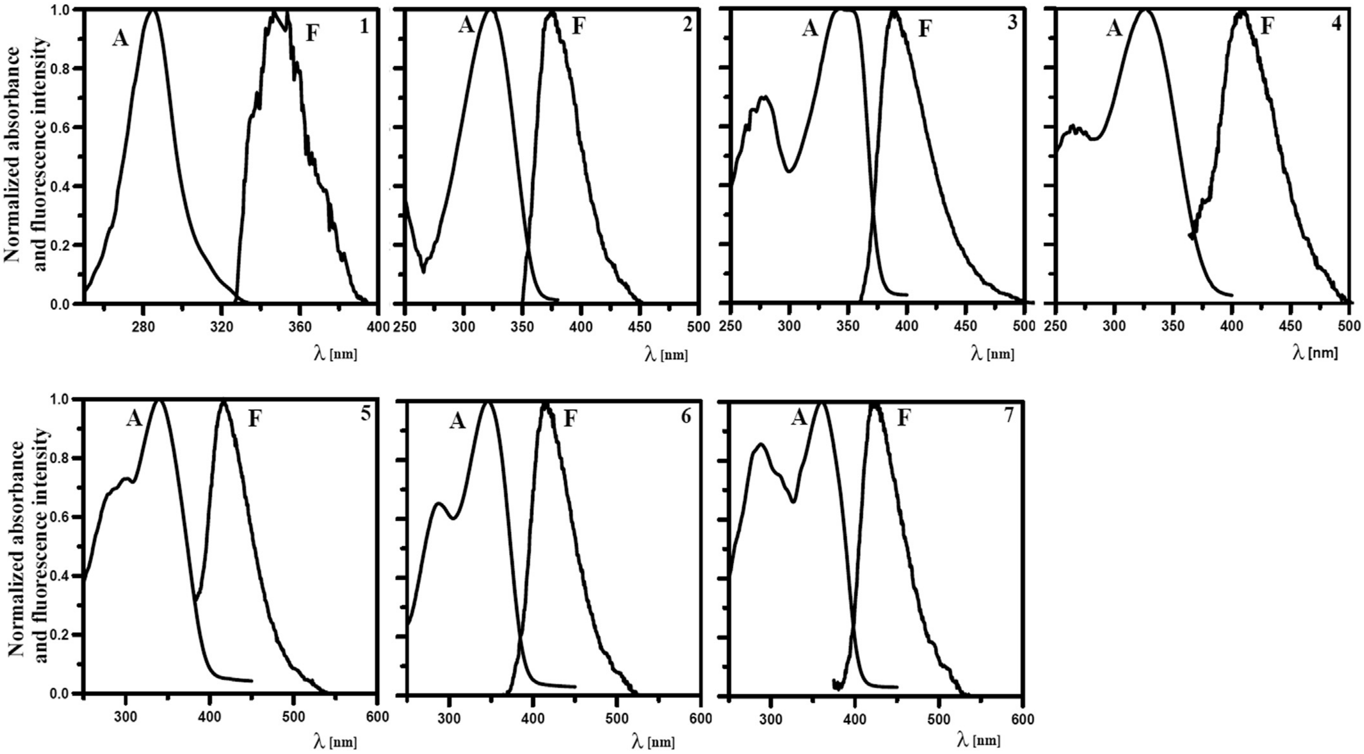

Fig. 1. Absorption (A) and fluorescence (F) spectra of **1**–**7** in DBE.

maxima). This splitting is more evident by considering biphenyl (**2b**) as starting compound for the series A. Both series show a clear convergence of the λ_{max} values with increasing n: the increment $\Delta\lambda$ is 38 nm between **2** and **1** and only 3 nm between **4** and **2**; $\Delta\lambda$ is 65 nm between **3** and **1** and only 10 nm between **7** and **3**. Chromophores **5** and **6** are structurally isomeric which is reflected by their close λ_{max} positions and represent a cross-section between structurally homogeneous series A or B. As the absorption maxima of chromophores **1**–**7** are practically independent on the solvent polarity (Table 2), all the aforementioned relationships are valid regardless the solvent used.

To better understand the relationships between the structure and the electronic spectra of **1**–**7**, their equilibrium conformation and the electronic excited state characteristics have been calculated using the semi-empirical AM1 procedure and INDO/S method with modified Nishimoto–Mataga gamma integrals as implemented in WinMOPAC 2.0 Package. For optimized geometry, the dihedral angle C(CH_3)–N–C(phenyl)-C(phenyl) (angle α, Fig. 2) was found 18° for all studied compounds. While are the hydrocarbon skeletons of compounds **1**, **3**, and **7** planar, the dihedral angles between 1,4-phenylene units of biphenyl and terphenyl linkers are 40 ± 1° in compounds **2**, **4**, **5**, and **6.** The position of the absorption maxima corresponds well with the molecular length and with the number of nodal planes. Compound **4** with two nodal planes absorbs at the same wavelength as shorter **2** with only one nodal plane. Middle-sized planar chromophore **3** absorbs at longer wavelength than **4** (two nodal planes) and even **5** and **6** (one nodal plane). As expected, compound **1** absorbs at the shortest wavelengths while the largest and fully planar compound **7** absorbs at the longest wavelength.

Table 2
Absorption and fluorescence maxima (nm) and the Stokes shifts ($\Delta\nu$, 10^3 cm^{-1}) of compounds **1**–**7**.

Comp.	DBE			EtAc			MeCN		
	λ^A	λ^F	$\Delta\nu$	λ^A	λ^F	$\Delta\nu$	λ^A	λ^F	$\Delta\nu$
1	285	349	6.43	286	350	6.39	288	353	6.48
2	323	374	4.22	326	398	5.55	328	422	6.79
3	350	390	2.93	350	428	5.21	352	478	7.59
4	326	409	6.26	331	447	7.94	333	498	9.95
5	339	417	5.52	345	461	7.29	348	538	10.15
6	346	415	4.81	349	466	7.19	351	540	9.94
7	360	424	4.19	362	480	6.79	362	552	9.51

Theoretical characteristics of the first two INDO/S electronic singlet transitions for optimized geometries of **1**–**7** are listed in Table 3. The intense absorption band of all studied compounds, except **1**, corresponds to “pure” HOMO–LUMO allowed transition and has π–π* nature. For compound **1**, the first transition is strictly forbidden and consists from σ–π* configurations with σ–MO localized on the phenylacetylene fragment. The second transition has a medium high oscillator strength and is strongly mixed by the HOMO–LUMO and σ–σ* (26–32) transitions localized on the acetylenic group. Likewise for **2**, the HOMO–LUMO transition appears as the second one, but in contrast to **1,** shows high “purity” and very high oscillator strength. The first transition of **2** consists from several π–π* configurations. For the remaining compounds **3**–**7**, the first electronic transition consists solely from the HOMO–LUMO configuration. The second transition for **3**, **5**, **6**, and **7** is formed by σ–π* configuration with σ–MO localized on the diphenylacetylene fragment while the second transition of **4** is formed by several π–π* configurations.

The allowed singlet transitions with the main HOMO–LUMO configuration are spectroscopically most important. The HOMO of all studied compounds is spread over the π-linker and *N*,*N*-dimethylanilino moiety dominantly. Several nodal planes appeared between the phenyl rings and triple bonds. Whereas in **1** is the LUMO localized mainly on the hydrocarbon skeleton, in **2**–**7** is spread over a whole π-system apart from the *N*,*N*-dimethylanilino moiety. Simultaneously, a strong π-bonding has been found between the particular phenyl rings (**2**, **4**–**6**) and between the phenyl and acetylenic groups (**1**–**7**) (Fig. 3).

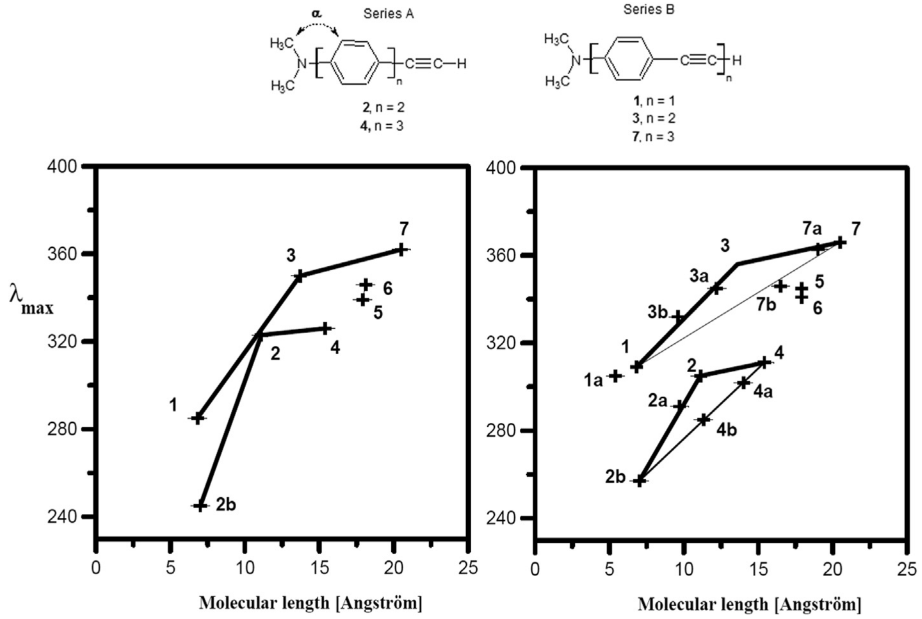

Fig. 2. Series A and B (above) and the dependence of the experimental (DBE, left) and theoretical (HOMO–LUMO configuration, right) absorption maxima [nm] on the molecular length.

The shapes of the HOMO, LUMO, and excited states dipole moments correspond well with the expected moderate charge-transfer (CT) character of the allowed electronic transitions accompanied by a partial electron transfer from the donor *N*,*N*-dimethylamino group (**1**) or from the *N*,*N*-dimethylanilino moiety (**2**–**7**) to the appended π-linker (Fig. 3). Hence, a π-linker, which consists of 1,4-phenylene and acetylenic units and possesses electronegative sp^2/sp carbons, can be considered as a weak acceptor. This observation is in agreement with previous findings [15,20–22,24]. The agreement of the theoretical electronic transitions, characterized by the high oscillator strength and by the predominant HOMO–LUMO CI configuration, with the experimental absorption maxima of **3**, **5**, **6**, and **7** is within the limit of ±6 nm. The calculated maxima for **2** and **4** are shifted hypsochromically by 17/15 nm which can be caused by AM1 description of their twisted biphenyl and terphenyl π-linkers. Changing the torsion angle between two phenyl rings of **2** by ±10° from that of equilibrium structure (39°) affects the first allowed transition (HOMO–LUMO) only by +5 nm for $\gamma = 29°$ and −8 nm for $\gamma = 49°$. The electronic transitions of **1** are strongly mixed by $\pi-\pi^*$ and $\sigma-\pi^*$ configurations. Hence, any assignment of the theoretical values to the spectrum is somewhat problematic. The theoretical value for this compound is shifted bathochromically compared to the experimentally obtained one.

Table 3
INDO/S theoretical spectral characteristics of S_0–S_i transitions of studied compounds.

Comp.	State	λ^{theor} [nm]	*f*	Main CI configuration	DM (Dipole moment) (Debay) Exc. st.	G. st.	λ^{exp} [nm] (in DBE)
1	1	342	0.000	26–29 (0.61) 26–31 (0.53)			
	2	309	0.222	28–29 (0.64) 26–32 (0.55)	2.9	2.0	285
2	1	306	0.042	42–45 (0.61)			
	2	304	1.032	42–43 (0.95)	7.1	2.2	323
3	1	356	1.186	46–47 (0.92)	5.7	2.4	350
	2	333	0.200	44–47 (0.91)			
4	1	311	1.661	56–57 (0.95)	9.1	2.2	326
	2	306	0.043	Strongly mixed			
5	1	345	1.910	60–61 (0.94)	4.7	2.4	339
	2	327	0.008	57–61 (0.84)			
6	1	341	1.992	60–61 (0.95)	8.5	2.4	346
	2	317	0.003	57–61 (0.75)			
7	1	366	2.341	64–65 (0.94)	7.4	2.5	360
	2	331	0.003	61–65 (0.65)			

Fig. 2 (right) shows a dependence of the theoretical electronic transitions of **1**–**7** on the molecular length. For a detailed analysis of the observed splitting, theoretical L_a transitions of less-substituted complementary compounds **1a**, **2a**–**b**, **3a**–**b**, **4a**–**b**, and **7a**–**b** have been included as well (for their structures see Table 1). It is obvious that biphenyl (**2b**) would represent a fundamental skeleton for the hydrocarbon series **2b**, **2a**, and **4a** and subsequently also for the sequence **2b**, **2**, and **4** (series A). On the other hand, ethynylbenzene (**1a**) seems to be a fundamental system for the hydrocarbon sequences **1a**, **3b**, and **7b** and **1a**, **3a**, and **7a** as well as for *N*,*N*-dimethylamino-substituted series **1**, **3**, and **7** (series B). Similarly to the experimental data (Fig. 2, left), compounds **5** and **6** do not fit in the aforementioned sequences and represent rather a cross-section between both series. However, both experimental and calculated λ_{max} values correlate well with the increasing molecular length and showed the same trends.

4. Fluorescence spectra and fluorescence quantum yields

In contrast to the absorption maxima, the fluorescence ones are bathochromically shifted monotonously by going from **1** to **7** (Table 2, Fig. 4 left). While the positions of the absorption maxima are influenced by the solvent polarity, the fluorescence maxima (except for **1**) show a strong bathochromic shift. A hint of convergence of fluorescence maxima with molecular length is apparent.

Since there are more factors that affect the Stokes shift (SS), e.g. a change of the molecular geometry during excited state life time, the excited state dipole moment, the solvent polarity, an analysis of the SS related to the molecular structure is rather complicated. Nevertheless, when comparing pair of chromophores, e.g. **2** with **4**

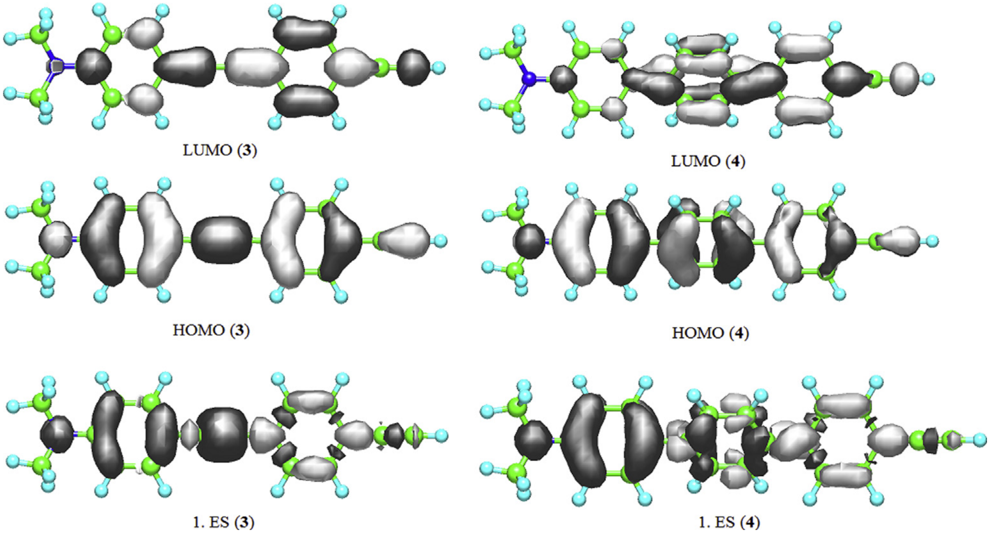
LUMO (3) LUMO (4)
HOMO (3) HOMO (4)
1. ES (3) 1. ES (4)

Fig. 3. The HOMO/LUMO visualizations and the electron displacement in the first electronic excited states (1. ES) for the compounds **3** and **4**.

and **3** with **7**, larger SS for **4** and **7** were found, this could be caused by higher transition dipole moments for **4** and **7**. This observation can be rationalized by the higher excited state dipole moments of **4** and **7**. The obvious difference in the SS between similar compounds **3** and **4** can be attributed to their very different molecular structure. While **3** is fully planar, **4** has two nodal planes and approximately twice greater excited state dipole moment. Compound **1** exhibited the highest SS (6430 cm^{-1}) in non-polar DBE. This compound has practically the same dipole moment in the ground and excited states. Moreover, no influence of the solvent polarity on its absorption and fluorescence maxima was found. The graphical representation of the dependence of the SS on the molecular length and the solvent polarity (Fig. 4, right) provides an interesting picture. The data are split again into two series: **1**, **2**, and **3** and **H**, **4**, **5**, **6**, and **7** where **H** represents a hypothetical molecule with the length similar to **1** that features much higher SS ($10–11 \times 10^3\ \mathrm{cm}^{-1}$) and absorption and fluorescence independent on the solvent polarity. However, despite our attempts to find such molecule, the structure of **H** remained unknown.

Table 4 shows the measured fluorescence quantum yields (q_F) of chromophores **1**–**7**. It is obvious that q_F of **1** is exceptionally low which can be due to the strong mixing of $\pi–\pi^*$ and $\sigma–\sigma^*$ configurations in the fluorescent state. The fluorescent states of **2**–**7** consist solely from HOMO–LUMO ($\pi–\pi^*$) configurations and their q_F is relatively high ranging from 0.41 to 0.90 (DBE), 0.20–0.58 (EtAc), 0.12–0.55 (MeCN), and 0.30–0.62 (DO). Similar to the absorption maxima, nearly linear dependence of the q_F on the molecular length for the series of planar compounds **1**, **3**, and **7** was found. While q_F increases with the molecule elongation, it decreases with increasing the solvent polarity. For instance, the q_F values of **3** and **7** decreases within the range of $0.41 \rightarrow 0.20 \rightarrow 0.12$ and $0.75 \rightarrow 0.46 \rightarrow 0.20$ respectively when going from DBE→EtAc→MeCN. This may be caused by an increase of a radiationless decay rate constant within the fluorescence bathochromic shift (stabilization of emitting excited state) regulated by the classical “energy gap law” [31]. A nonradiative process, probably internal $S_1–S_0$ conversion, could be responsible for the fluorescence quenching. However, no relationships between the structure, $q_{F,}$ and solvent polarity were found for non-planar systems having one (**2**, **5**, and **6**) or two (**4**) nodal planes. On the contrary to planar chromophores **3** and **7**, twisted molecules **2** and **4**–**6** showed generally higher q_F with a diminished influence of the solvent polarity. An interplay of the energy, geometry, and electronic structure of the fluorescent state plays evidently most important role in its deactivation mechanism, consequently in fluorescence quenching.

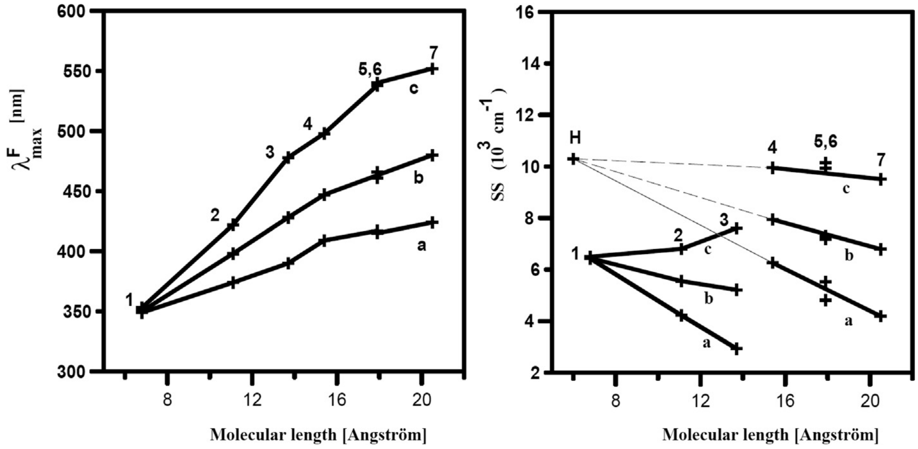

Fig. 4. Dependence of the fluorescence maxima (left) and the Stokes shift (right) on the molecular length of **1**–**7** measured in DBE (a), EtAc (b) and MeCN (c). **H** denotes a hypothetical compound.

Table 4
Measured fluorescence quantum yields.

Comp.	q_F			
	DBE	EtAc	MeCN	DO
1	0.09	0.054	0.034	0.07
2	0.90	0.58	0.55	0.59
3	0.41	0.20	0.12	0.30
4	0.69	0.44	0.41	0.52
5	0.82	0.36	0.30	0.57
6	0.70	0.48	0.46	0.62
7	0.75	0.46	0.20	0.56

5. Conclusion

Seven *N*,*N*-dimethylamino-substituted phenyleneethynylene oligomers with systematically extended and varied π-conjugated systems were prepared and further studied by absorption and fluorescence spectra as well as calculations. The π-linker separating *N*,*N*-dimethylamino donor and terminal acetylene moiety consists of a combination of one to three 1,4-phenylene and none to two acetylenic subunits. These molecules represent a comprehensive series of model D–π compounds as a part of the more common D–π–A push–pull chromophores and are intended to study fundamental structure–property relationships. Measured and calculated properties were correlated with structural features of **1**–**7** and following conclusions can be made:

- the molecular length was proved to be the fundamental structural factor affecting spectral properties of linear compounds such as **1**–**7**;
- beside the molecular length, the spectral properties were also significantly influenced by the molecule planarity;
- the most bathochromically shifted bands of **1**–**7** have CT character and correspond to HOMO → LUMO transition;
- a π-conjugated system consisting of 1,4-phenylene and acetylenic units behave as weak electron acceptor due to the presence of more electronegative sp^2/sp carbons;
- non-planar molecules showed the largest changes in the dipole moment between the ground and excited states;
- the fluorescence maxima are shifted bathochromically with increasing molecular length;
- for fully planar molecules **3** and **7** were the fluorescence quantum yields significantly decreased with the increasing solvent polarity;
- the influence of the solvent polarity on the q_F is diminished for non-planar molecules **2** and **4**–**6**;
- the observed Stokes shifts mimic the size of the molecule.

In view of the current interest in novel organic π-conjugated materials and their growing applications in optoelectronic devices, we believe that this study would serve as useful guide to design such organic molecules.

Acknowledgment

This research has been supported in part by the Czech Science Foundation (13-01061S) and in part by the Czech Ministry of Education, Youth and Sports (Aktion 63p20).

References

[1] Forrest SR, Thompson ME. Special issue on organic electronics and optoelectronics. Chem Rev 2007;107:923–1386.

[2] Miller RD, Chandross EA. Special issue on materials for electronics. Chem Rev 2010;110:1–574.

[3] He GS, Tan LS, Zheng Q, Prasad PN. Multiphoton absorbing materials: molecular design, characterization and application. Chem Rev 2008;108:1245–330.

[4] Diederich F, Stang PJ, Tykwinski RR, editors. Acetylene chemistry. Weinheim, Germany: Wiley-VCH; 2005. pp. 51–99.

[5] Haley MM, Tykwinski RR, editors. Carbon-rich compounds. Weinheim, Germany: Wiley-VCH; 2006.

[6] Weder C. Poly(aryleneethynylene)s. From synthesis to application. Adv Polym Sci 2005;177:1–248.

[7] Bunz UHF. Poly(aryleneethynylene)s: synthesis, properties, structures, and applications. Chem Rev 2000;100:1605–44.

[8] Li C, Liu M, Pschirer NG, Baumgarten M, Müllen K. Polyphenylene-based materials for organic photovoltaics. Chem Rev 2010;110:6817–55.

[9] Silvestri F, Marrocchi A. Acetylene-based materials in organic photovoltaics. Int J Mol Sci 2010;11:1471–508.

[10] Egbe DAM, Birckner E, Klemm E. Highly luminescent diyne ($-C\equiv C-C\equiv C-$) containing hybrid polyphenyleneethynylene/poly(*p*-phenylenevinylene) polymer: synthesis and characterization. J Polym Sci A Polym Chem 2002;40:2670–9.

[11] Breen CA, Tischler JR, Bulović V, Swager TM. Highly efficient electroluminescence from poly(phenylene ethynylene) via energy transfer from hole-transport matrix. Adv Mater 2005;17:1981–5.

[12] Hoppe H, Egbe DAM, Mühlbacher D, Sariciftci NS. Photovoltaic action of conjugated polymer/fullerene bulk heterojunction solar cells using novel PPE–PPV copolymers. J Mater Chem 2004;14:3462–7.

[13] McQuade DT, Pullen AE, Swager TM. Conjugated polymer-based chemical sensors. Chem Rev 2000;100:2537–74.

[14] Fillaut JL, Andriès J, Perruchon J, Desvergne JP, Toupet L, Fadel L, et al. Alkynyl ruthenium colorimetric sensors: optimizing the selectivity toward fluoride anion. Inorg Chem 2007;46:5922–32.

[15] Kivala M, Diederich F. Acetylene-derived strong organic acceptors for planar and nonplanar push–pull chromophores. Acc Chem Res 2009;42:235–48.

[16] Ali SM, Tedford CE, Gregory R, Handley MK, Yates SL, Hirth WW, et al. Design, synthesis, and structure–activity relationships of acetylene-based histamine H_3 receptor antagonist. J Med Chem 1999;42:903–9.

[17] Senior SJ, Illarionov PA, Gurcha SS, Campbell IB, Schaeffer ML, Minnikin DE, et al. Acetylene-based analogues of thiolactomycin, active against *Mycobacterium tuberculosis* mtFabH fatty acid condensing enzyme. Bioorg Med Chem Lett 2004;14:373–6.

[18] Bureš F, Schweizer WB, Boudon C, Gisselbrecht JP, Gross M, Diederich F. New push–pull chromophores featuring TCAQ (11,11,12,12-tetracyano-9,10-anthraquinodimethane) and other dicyanovinyl acceptors. Eur J Org Chem; 2008:994–1004.

[19] Kulhánek J, Bureš F. Imidazole as a parent π-conjugated backbone in charge-transfer chromophores. Beilstein J Org Chem 2012;8:25–49.

[20] Bureš F, Schweizer WB, May JC, Boudon C, Gisselbrecht JP, Gross M, et al. Property tuning in charge-transfer chromophores by systematic modulation of the spacer between donor and acceptor. Chem Eur J 2007;13:5378–87.

[21] Bureš F, Čermáková H, Kulhánek J, Ludwig M, Kuznik W, Kityk IV, et al. Structure–property relationships and nonlinear optical effects in donor-substituted dicyanopyrazine-derived push–pull chromophores with enlarged and varied π-linkers. Eur J Org Chem; 2012:529–38.

[22] Kirketerp MBS, Petersen MÅ, Wanko M, Zettergren H, Rubio A, Nielsen MB, et al. Double-bond versus triple-bond bridges: does it matter for the charge-transfer absorption by donor–acceptor chromophores? ChemPhysChem 2010;11:2495–8.

[23] Liu B, Zhang HL, Liu J, Huang ZL, Zhao YD, Luo QM. Acetylene-substituted two-photon absorbing molecules with rigid elongated pi-conjugation: synthesis, spectroscopic properties and two-photon fluorescence cell imaging applications. J Fluoresc 2007;17:573–9.

[24] Kulhánek J, Bureš F, Pytela O, Mikysek T, Ludvík J, Růžička A. Push–pull molecules with a systematically extended π-conjugated system featuring 4,5-dicyanoimidazole. Dyes Pigm 2010;85:57–65.

[25] Tykwinski RR, Gubler U, Martin RE, Diederich F, Bosshard C, Günter P. Structure–property relationships in third-order nonlinear optical chromophores. J Phys Chem B 1998;102:4451–65.

[26] Egbe DAM, Carbonnier B, Birckner E, Grummt UW. Arylene-ethynylene/arylene-vinylene copolymers: synthesis and structure–property relationships. Prog Polym Sci 2009;34:1023–67.

[27] Hlel A, Mabrouk A, Chemek M, Alimi K. Theoretical study of phenylene–thiophene oligomers: structure–properties relationship. Spectrochim Acta Part A 2012;99:126–35.

[28] Ayachi S, Ghomrasni S, Bouachrine M, Hamidi M, Alimi K. Structure–property relationships of soluble poly(2,5-dibutoxyethoxy-1,4-phenylene-alt-2,5-thienylene) (PBuPT) for organic–optoelectronic devices. J Mol Chem 2013;1036:7–18.

[29] Birks JB, Dyson DJ. The relations between the fluorescence and absorption properties of organic molecules. Proc R Soc A 1963;275:135–48.

[30] Kulhánek J, Bureš F, Ludwig M. Convenient methods for preparing π-conjugated linkers as building blocks for modular chemistry. Beilstein J Org Chem 2009;5:11.

[31] Avouris P, Gelbart WM, El-Sayed MA. Nonradiative electronic relaxation under collision-free conditions. Chem Rev 1977;77:793–833.